Investigation of low-energy electronic excitations in quasi-one-dimensional Ising antiferromagnet CsFeCl$_3$·2H$_2$O via Raman spectroscopy

V. S. Kurnosov

B. Verkin Institute for Low Temperature Physics and Engineering of the National Academy of Sciences of Ukraine
Kharkiv 61103, Ukraine
E-mail: kurnosov@ilt.kharkov.ua

The frequencies of low-lying electronic excitations in the quasi-one-dimensional antiferromagnet CsFeCl$_3$·2H$_2$O were determined by Raman spectroscopy. The lowest of them (57 cm^{-1}) was attributed to the magnon-like excitation of the chain of Ising spins of paramagnetic Fe^{2+} ions. And the next one (77 cm^{-1}) can most likely be attributed to the exciton-like one, associated with the electronic transition to the lower level of the excited orbital quasi-doublet d_{zx}, d_{zy} split by the spin-orbit interaction. Investigations of the splittings and shifts of Raman lines in an external magnetic field allowed us to estimate the values of the magnetic moments of the sublattices in the ground state and to determine their spatial orientation relative to the crystallographic directions.

Keywords: magnon, exciton, Ising spin chain, quasi-one-dimensional antiferromagnet.

1. Introduction

Orthorhombic crystals with the chain-like arrangement of paramagnetic ions having total chemical formula AMX$_3$·2H$_2$O (A = Cs, Rb, M = Mn, Fe, Co, X = Cl, Br) were an object of extensive research by both experimentalists and theoreticians due to their quasi-one-dimensional magnetism. Some of them (CsCoCl$_3$·2H$_2$O, CsMnCl$_3$·2H$_2$O, CsMnBr$_3$·2H$_2$O, α-RbMnCl$_3$·2H$_2$O, CsFeCl$_3$·2H$_2$O, and RbFeCl$_3$·2H$_2$O) are isomorphs and have D_{2h}^8 (Pcca) symmetry in the paramagnetic state [1–3]. The unit cell contains 4 formula units. Depending on a divalent paramagnetic ion, quasi-one-dimensional antiferromagnetic structures with different types of exchange anisotropy are realized: from purely Heisenberg [Mn^{2+}, $3d^5$, $^6A_{1g}$ (^6S)] to close to purely Ising [Fe^{2+}, $3d^6$, $^5F_{2g}$ (^5D), Co^{2+}, $3d^7$, $^5F_{1g}$ (^4F)] [1, 4, 5]. All members of this crystal family, except for Mn-containing ones, exhibit canting of sublattices. This is not surprising, taking into account their structure features (Fig. 1). Ions Fe^{2+} and Co^{2+} with the nonsinglet orbital ground state due to spin-orbit interaction "feel" the relative deformation of the octahedral environment of the ligands consisting of halogens and oxygen atoms of crystalline hydrate water. The magnetic moment direction can be either along or normal to the local twofold axis c_{2b} which determines the symmetry of the position of the paramagnetic. For the Mn-containing compounds, the first type of

orientation takes place [5–7], and for Fe- and Co-containing compounds, the second [1, 4, 8, 9]. The main superexchange interaction occurs in the chains ···Cl1−M–Cl1−M···, i.e., along crystal axis a. Exchange interactions in other directions b and c are much weaker, which determines a quasi-one-dimensionality of the magnetic structures of this crystal family. The chains of magnetic ions are quite well isolated
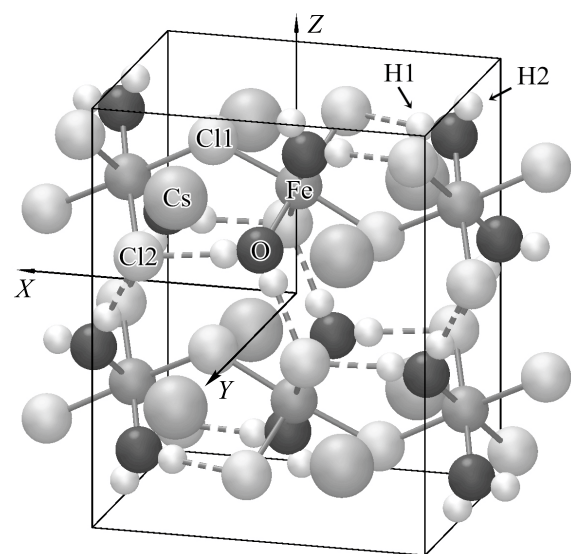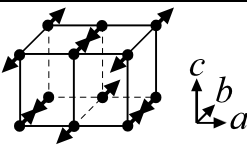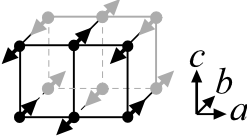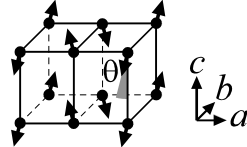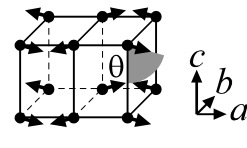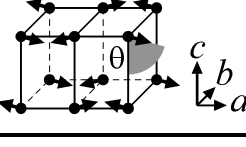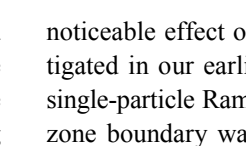

Fig. 1. Structure of CsFeCl$_3$·2H$_2$O at 4.2 K according to [1]. Hydrogen bonds H–Cl2 are shown by dashed lines.

in perpendicular directions. Along *c* chains are connected via hydrogen bonds, and in the *b* direction chains are separated by layers of alkali ions. These structural features are reflected on the mechanical properties of the crystals, which are easily cleaved along the (001) planes.

Magnetic 3D ordering occurs at different temperatures in different compounds, but the doubling of the magnetic cell in the *b* direction, which takes a place for most of the listed compounds, is typical (see Table 1). In the antiferromagnetic phases of the crystals with M = Fe, Co within individual chains, a mutual tilt of the neighbor spins due to the Dzyaloshinskii–Moriya interaction leads to the appearance of an uncompensated ferromagnetic moment. In Fe-containing crystals, the nonzero projection of the moment is M_z, while in Co-containing ones, M_x. Nevertheless, the full moment remains zero due to alternation of its direction in the neighboring chains (see Table 1). By applying external magnetic fields along the indicated directions for the corresponding crystals, the I-order phase transitions (PT) into the ferrimagnetic (canted antiferromagnetic) state can be induced [1, 8, 9]. A characteristic feature of the phase transition is that the flip of all spins in the chain occurs as a result of the motion of the magnetic soliton, the boundary between the segments of the chain with the opposite direction of the ferromagnetic moment. Moreover, in RbFeCl$_3$·2H$_2$O (RFC) and CsFeCl$_3$·2H$_2$O (CFC) this PT occurs with passage through a sequence of metastable intermediate phases, which are characterized by a different ratio of the numbers of chains with the orientation of the ferromagnetic moment along and against the external magnetic field [1, 4, 9].

Table 1. Magnetic structures of some isostructural orthorhombic AMX$_3$·2H$_2$O compounds: θ is an angle between sublattice magnetic moments and the axis *c* in the *ac* plane

Compound	Magnetic symmetry	Magnetic structure	θ, deg	T_N, K	Ref.
CsMnCl$_3$·2H$_2$O	$P_{2b}c'ca'$			4.89	[6]
α-RbMnCl$_3$·2H$_2$O			–	4.56	[7]
CsMnBr$_3$·2H$_2$O	$Pc'c'a'$			5.75	[5]
CsCoCl$_3$·2H$_2$O	$P_{2b}cca'$		10	3.38	[8]
CsFeCl$_3$·2H$_2$O	$P_{2b}cca'$		75–78	12.75	[1, 4]
RbFeCl$_3$·2H$_2$O	$P_{2b}c'ca$		71–74	11.96	[1, 4]

Despite many experimental investigations of CFC related to its interesting magnetic properties, very few of them were carried out with optical methods. The only experiments we know about are studies of exciton light absorption in strong magnetic fields up to the values of the metamagnetic transition [10–12]. Far IR absorption was investigated in RFC [13].

Since all crystals of the presented family do not undergo structural phase transitions, and their structures are very similar, apparently, the study of their vibrational spectrum by Raman and IR spectroscopy methods did not arouse much interest, especially since the vibrational spectra of one of the representatives of this family, namely CsMnCl$_3$·2H$_2$O (CMC), have been studied in detail earlier [14–16]. The most noticeable effect of magnetic ordering in CFCs was investigated in our earlier work [17], where the provocation of single-particle Raman scattering by phonons of the Brillouin zone boundary was discovered, and a mechanism for this observation was proposed. Another interesting effect associated with the features of electronic Raman scattering in CFC, as well as data on its vibrational spectrum, have not been previously reported, which is the purpose of the present paper.

Despite the long history of research and the unlikely prospect of practical application, these crystals can find their place in modern studies of the effects associated with the quasi-one-dimensionality of these magnetic structures [18].

2. Experimental

A detailed description of the sample preparation and experimental procedure was done elsewhere, in our earlier paper [17]. The actual temperature in the sample volume irradiated by the laser source in Raman experiments was measured using the well-known relationship between the Stokes I_s and anti-Stokes I_a intensity of single-particle phonon scattering with frequency ω: $k_B T = \hbar\omega/\ln\left(I_s/I_a\right)$, where k_B is the Boltzmann constant. Later, the Raman polarization is labeled using Porto S.P.S. notation [19] like $a(BC)d$, where a and d denote direction of the wave-vectors of the incident and scattered light, and B and C the direction of their polarization (when the direction of the wave-vectors is not important, short designations like BC are also used, corresponding to the components of the Raman tensor).

3. Phonon spectrum

In the structure of CFC and CMC crystals, paramagnetic metal ions occupy a position with local symmetry 2 on the c_{2z} axis, the Cs^+ and $Cl(1)^-$ ions have the same local symmetry, but are located on the c_{2y} axes. All other ions are in a common position. Crystals contain water molecules. The frequencies of internal vibrations of a water molecule are well known: the deformation mode has a frequency of ~ 1600 cm^{-1}, and the valence symmetric and antisymmetric modes are in the range of ~ 3400 cm^{-1}. Such high frequencies allow using an approximation where the internal vibrations of these molecules are considered sufficiently isolated from the rest of the phonon spectrum. The fundamental vibrations of the crystal lattice now can be described by the displacements of individual ions and water molecules, the rotations of water molecules and their internal vibrational degrees of freedom. According to the previous studies [14, 15], the vibrational spectrum of the crystals can be separated in frequencies as follows: the range 0–400 cm^{-1} belongs to vibrations without regard to the internal structure of aqua molecules, a range 400–800 cm^{-1} is occupied by hindered rotations (librations) of H_2O molecules, and their internal vibrations lie in the high-frequency range 1500–3500 cm^{-1}.

Also, among the structural elements of the lattice of these crystals, one can distinguish the cis-octahedra MCl_4O_2 with shared Cl1 vertices, which forms zigzag chains elongated in the a direction (Fig. 1). This feature allows us to introduce additional specifications in a description of the low-frequency range of vibrations, so-called "lattice range". Inside each unit cell, there are two chains, each of which consists of two MCl_4O_2 octahedra. It is logical to assume that the modes in which the shape of the octahedra undergoes minimal distortion will be predominantly low-frequency. These modes correspond to rotations of the octahedra about their free axes and translation of chains as a whole. Vibrations of "heavy" alkaline ions Cs^+ probably fall into the same frequency range [14], which is restricted to a frequency of ~ 100 cm^{-1} [15]. Accordingly, the range 100–400 cm^{-1}, hereinafter called "deformative", presumably includes the internal modes of the MCl_4O_2 octahedra. Table 2 shows a set of fundamental vibrations of the presented crystals in accordance with the above classification scheme.

The Raman spectra of the CFC crystal were studied in the temperature range 2–300 K. The absence of structural phase transitions in the paramagnetic state follows from the nature of their temperature evolution: the number of observed spectral lines and their polarization are retained. Changes in the Raman spectrum reflect only a gradual narrowing of the spectral lines and a slight increase in their frequencies with decreasing temperature (Fig. 2). In CMC, as was shown earlier [15], such a picture is also observed below T_N. From excitations which occur in CMC in magnetically ordered phase, the only two-magnon band was detected [20]. In CFC, the picture is more complex. All phonon excitations from the paramagnetic phase preserve their presence in the antiferromagnetic one. However, on their background, new bands appear at low temperatures. Some of them have been studied earlier [17].

Table 2. Vibrational modes of $CsMCl_3\cdot 2H_2O$ crystalls with lattice symmetry *Pcca*

Ion, molecule, complex	Mode	Vibrational representation*							
		A_g	B_{1g}	B_{2g}	B_{3g}	A_u	B_{1u}	B_{2u}	B_{3u}
Cs^+	Translational	1	1	2	2	1	1	2	2
MCl_4O_2 octahedra	Rotational	1	1		2	1	1		2
	Translational		1	1	1		1	1	1
	Internal	7	7	8	7	7	7	8	7
H_2O	Rotational	3	3	3	3	3	3	3	3
	Deformation	1	1	1	1	1	1	1	1
	Valent	2	2	2	2	2	2	2	2

* In mechanical representation, there are 3 acoustic modes, which are transform according to the representation
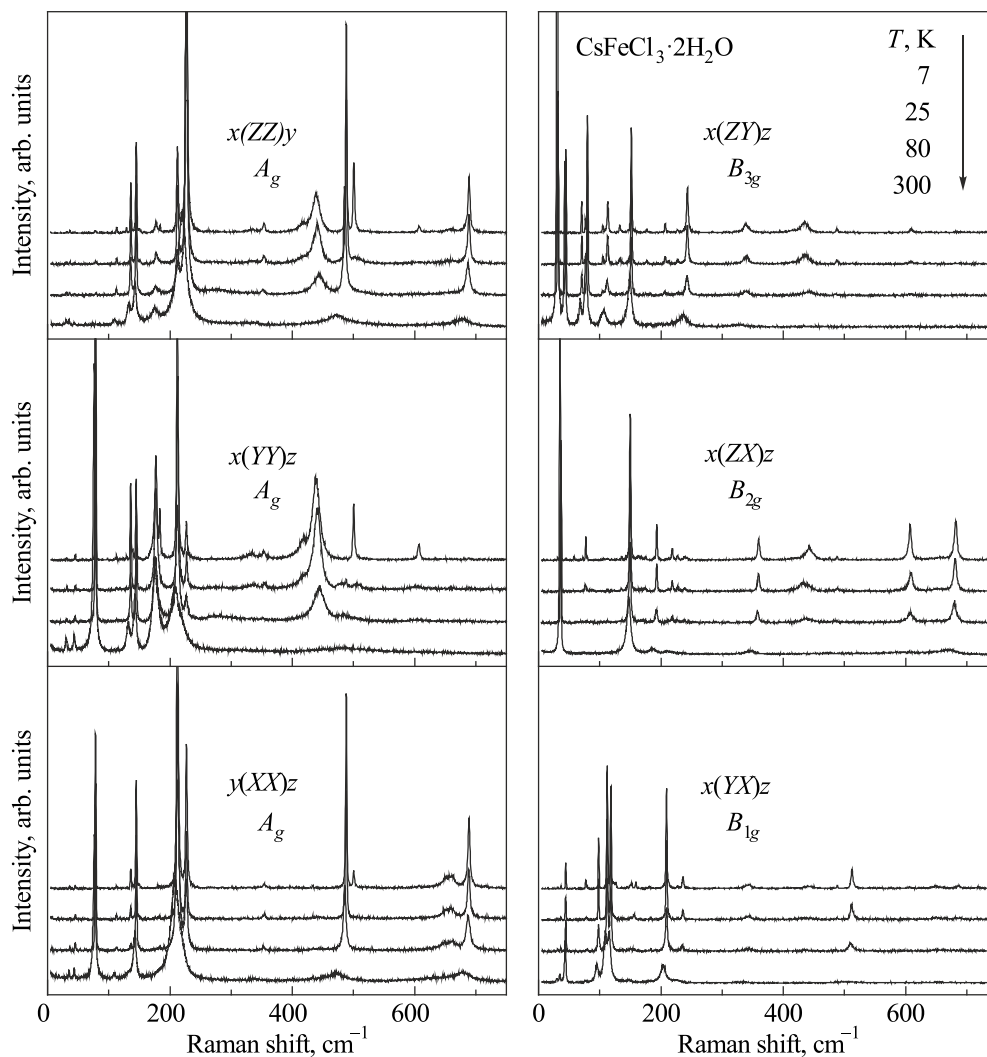$\Gamma_{ac} = B_{1u} + B_{2u} + B_{3u}$.

Fig. 2. Raman spectra of the $CsFeCl_3 \cdot 2H_2O$ single crystal at selected temperatures in the frequency range including the "lattice", "deformation" of $FeCl_4O_2$, and librational modes of H_2O. Temperatures, polarizations and mode symmetries (class *mmm*) are indicated for all groups of spectra. Spectral resolution 2 cm^{-1}.

Comparison between CFC and CMC spectra in the frequency range of lattice and deformation modes is presented in the Table 3. It should be noted that the table contains only modes of phonon nature. The asterisks mark the modes observed in the CFC in the magnetically ordered state. They refer to the phonon modes of the boundary of the paramagnetic Brillouin zone [17]. It should be noted that these Raman signals appear only in the *diagonal* components of the polarizability tensor.

Without taking into account the internal structure of the water molecules, the calculation gives $9A_g + 10B_{1g} + 11B_{2g} + 12B_{3g}$ vibrational modes active in the Raman scattering (see Table 2). Experimentally, $9A_g + 8B_{1g} + 9B_{2g} + 11B_{3g}$ and $9A_g + 9B_{1g} + 10B_{2g} + 11B_{3g}$ modes are observed in CFC and CMC, respectively, that is in good agreement with the group theory prediction. In the Raman spectrum of CFC with B_{1g} symmetry, the mode of the out-of-phase translational in c direction oscillations of the above-mentioned

chains of the crystal structure could not be detected. In the CMC crystal, this mode is observed as very weak line at the frequency about 67 cm^{-1}. Perhaps, for some reason, its polarizability in CFC is even lower, or it is masked by the leakage into the forbidden polarization of the rather intense B_{3g} band at 70.5 cm^{-1}.

In the low-frequency "lattice" range, where the theory predicts the presence of $2A_g + 3B_{1g} + 3B_{2g} + 5B_{3g}$ Raman-active modes (see Table 2), they are all observed in CMC, while in the CFC Raman spectrum two lines with estimative frequencies of 67 (B_{1g}) and 46 (B_{2g}) cm^{-1} are absent. Good coincidence of the number and symmetry of the predicted and observed lines in the Raman spectra of CMC and CFC indicates the adequacy of the presented model description of the vibrational spectrum of these crystals. As far as possible, the experimentally found complete Raman spectrum of phonon excitations facilitates the identification of excitations of another nature, for example, electronic or spin.

Table 3. Frequencies and assignment [14, 15] of low-frequency phonon modes in CFC and CMC crystals at some temperatures. Asterisks mark Brillouin zone boundary phonon modes provoking by magnetic ordering in CFC [17]

CMC, $T=2$ K	CFC, T, K				Mode symmetry	Assignment
	2	25	80	300		
Lattice modes						
30.2	31.3	31.4	31.4	30.5	B_{3g}	Chains translation along *a*
36.5	36.5	36.5	36.2	35.0	B_{2g}	Chains translation along *b*
43.9	44.4	44.4	44.4	43.5	B_{1g}	Librations of MCl$_4$O$_2$
43.9	44.6	44.6	44.4	43.0	B_{3g}	
44.2	45.3	45.2	45.1	43.5	A_g	
45.8	–	–	–	–	B_{2g}	
67.1	–	–	–	–	B_{1g}	Chains translation along *c*
68.9	70.5	70.7	70.7	67.9	B_{3g}	
75.9	79.9	79.9	79.8	77.4	B_{3g}	
75.1	78.4	78.4	78.2	76.5	A_g	
80.7	–	–	–	–	B_{2g}	
91.8	98.2	98.2	98.0	95.1	B_{1g}	
98.0	105.3	105.1	104.9	~103.3	B_{3g}	
Internal vibrations of MCl$_4$O$_2$ cis-octahedra in the chains						
100.6	113.0	112.7	112.4	109.1	A_g	
106.1	112.5	112.5	112.2	108.4	B_{2g}	
106.1	113.2	112.9	112.0	107.4	B_{3g}	
108.5	112.2	112.2	112.1	108.8	B_{1g}	
113.4	118.2	118.3	118.1	115.4	B_{1g}	
	123.7*	–	–	–	***A_g***	
	129.1*	–	–	–	***A_g***	
–	135.6	135.3	134.6	130.5	B_{2g}	
131.9	136.1	136.1	135.8	132.3	A_g	
	139.6*	–	–	–	***A_g***	
137.6	132.7	133.0	~132.4	–	B_{3g}	
137.6	145.0	145.0	144.9	142.8	A_g	
137.9	149.9	149.6	149.3	147.4	B_{2g}	
147.4	151.7	151.6	151.4	149.1	B_{3g}	
149.5	152.5	~150.3	150.8	147.5	B_{1g}	
164.5	175.0	173.9	171.5	168.9	B_{2g}	
164.5	177.2	177.0	176.3	175.3	A_g	
	183.9*	–	–	–	***A_g***	
189.8	193.2	193.2	192.4	186.5	B_{2g}	
198.7	207.0	206.9	206.2	199.0	B_{3g}	
206.7	212.4	212.4	212.3	207.9	A_g	
210.2	209.1	209.4	209.0	203.7	B_{1g}	
210.8	218.6	218.5	217.8	210.2	B_{2g}	
220.3	227.2	227.1	226.5	220.2	A_g	Valence vibrations M–Cl2
225.5	236.0	236.0	234.9	225.9	B_{1g}	
234.3	239.1	238.7	238.2	236.2	B_{2g}	
239.7	243.3	243.1	242.6	236.4	B_{3g}	
324.3	339.2	338.7	338.5	330.3	B_{3g}	Valence vibrations M–O
328.6	342.6	342.9	342.9	336.2	B_{1g}	
341.0	359.7	359.4	357.8	346.0	B_{2g}	
341.7	353.7	357.5	351.7	~337.5	A_g	

4. Electronic transitions in the Raman spectrum of CFC

The ground state of the Fe^{2+} ion in the octahedral coordination of the ligands is $^5T_{2g}(^5D)$ multiplet. In the CFC, according to estimates [21], the splitting in the $10Dq$ cubic field of the $^5T_{2g}$ triplet and ^5E_g doublet is about 10000 cm^{-1}. At that, the orbital ground triplet splits by the tetragonal part of the crystal field to d_{zx}, d_{zy} doublet and d_{xy} singlet with the energy of (685 ± 50) cm^{-1} in the structurally isomorphic RbFeCl$_3$·2H$_2$O. According to [21], the ground state is an orbital doublet split by the rhombic part of the crystal field into two singlets with energy difference of ~ 30 cm^{-1}. The spin-orbit* lifts the fivefold spin degeneracy of each of the orbital singlets of the ground state. As a result, 10 spin states overlap the energy range of about 330 см$^{-1}$. The ground state is a quasi-doublet with a splitting $\delta \leq 0.5$ cm^{-1}, the first excited single-ion state has an energy of ~ 50 см$^{-1}$, the next one, ~ 90 cm^{-1}. Estimates of the lowest electronic, excitonic (magnon) excitations in RbFeCl$_3$·2H$_2$O and CFC bring to similar values [11–13].

Two quasi-degenerated singlets in the ground state of the Fe^{2+} ions in the paramagnetic state enable some authors to describe the considered compound in the Ising model with an effective spin $S_{eff} = 1/2$ and a g-factor in the range 9.2–9.6 [13, 21]. Other authors [10–12] proceed from the triplet structure of the ground state, where the doublet with $j_a = \pm1$ projection of the total angular momentum onto the quantization axis a possesses the lowest energy, and the first excited state is the singlet $j_a = 0$. In the antiferromagnetic phase, the ground state energy levels split under the action of exchange interaction with neighboring sites. In the Ising model, the elementary excitation over the ground Néel state is a state with one "inverted" spin. Taking into account the interaction only with neighboring sites, the energy of this state is $E_{ex} = 2J_a S^2 z$, where J_a is the exchange constant of the interaction of neighbors, S is the spin, the projection of which can have only two values $S_a = \pm S$, z is the number of exchange-coupled neighbors. For a one-dimensional chain, $z = 2$; therefore, for the effective Ising spin 1/2 the excitation energy of the magnon is $E_{ex} = J_a$. In the CFC, the exchange constant has the value $J_a = (58 \pm 7)$ cm^{-1} [9]. It should be noted that the values of the exchange integrals in the cited papers are half as much, which follows from the notation of the exchange term in the spin Hamiltonian. For isostructural RbFeCl$_3$·2H$_2$O, according to the data of various experiments, this value varies in the range 54–63 cm^{-1} [13]. At that, the energy of the lowest electronic excitation observed in the IR spectra is 49.7 cm^{-1} [13].

4.1. Model of low-energy electronic levels of Fe^{2+} in CFC

Due to the proximity of the ground state in CFC and RbFeCl$_3$·2H$_2$O to the Ising one, they exhibit metamagnetic properties. As mentioned above, each chain in CFC contains two equivalent Fe^{2+} ions, which are belong to two sublattices and are characterized, respectively, by two magnetic vectors: $\mathbf{L} = \mathbf{S}_1 - \mathbf{S}_2$ and $\mathbf{M} = \mathbf{S}_1 + \mathbf{S}_2$. Only the L_a and M_c projections have a nonzero value within the frame of the magnetic symmetries that are realized in these compounds (see Table 1). An external magnetic field directed along the a axis leads to a metamagnetic phase transition, as a result of which the antiferro- and ferromagnetic vectors become swapped. In the spin-flip phase $L_c \neq 0$ and $M_a \neq 0$ (magnetic symmetry $Pc'c'a$). This transition was observed from the field dependence of the absorption spectra and from the magnetization at 4.2 K [10, 22]. In the opinion of the authors of [10, 22], the transition is accompanied by the formation of an interphase boundary; therefore, it is of the first order, while no noticeable hysteresis was found.

The ferromagnetic moments M_c of single chains in the bc plane produce an antiferromagnetic structure consisting of four such moments. A significant difference in the values of interchain and intrachain exchange (by more than an order of magnitude) is reflected in the values of the critical fields at which metamagnetic transitions occur when a field is applied along the a and c axes. If $H_{a\,cr} \approx 140$ kOe [10, 22], then $H_{c\,cr} \approx 10$ kOe [1, 4]. Moreover, for $\mathbf{H} \parallel c$ at the temperatures much lower than T_N, a two-step behavior of magnetization is observed, which is characterized by the intersection of two critical lines $H_{c1}(T)$ and $H_{c2}(T)$ in the H_c–T phase diagram [4]. These lines divide the phase plane onto three regions: antiferromagnetic (AF), ferrimagnetic (FI), and ferromagnetic (F). The names are arbitrary and characterize the ordering of the moments M_c of the chains. It is characteristic that value of magnetization in the FI phase is half the value in the F phase $M_{cFI} = \frac{1}{2} M_{cF}$ [1, 4]. Consequently, it is characterized by a flip of only half of the chains with the $-M_c$ projection of the magnetic moment in the AF structure onto the positive direction of the external magnetic field.

"Flipped" chains can form ordered or disordered structures, depending on their proportion with respect to the unperturbed structure. Calculations carried out in [4] showed a large number of possible intermediate phases in the range of field values 0–H_{c2}, switching between which is accompanied by jumps in magnetization. The most significant of the jumps relates to the critical field H_{c1}.

---

* The constant of spin-orbit interaction for Fe^{2+} has the order of -115 K or -80 cm^{-1}.

The observation of the jumps is possible in the narrow temperature range, since the switching of the chain magnetization $-M_c \rightarrow +M_c$ can't occur only due to the overturn of vector **M**, but is associated with the sign change of L_a of entire chain. This requires thermally activated nucleation of a domain within a chain with an opposite orientation of the vector **L**. The energy of such excitation is $E_{ex} = J_a$, the energy of one "flipped" spin. Further, as it is easy to see, this excitation splits into two kinks with equivalent (disregarding interactions with neighboring chains) energy, which, moving in opposite directions, "flip" spins of the entire chain. The probability of populating this state is proportional to $\exp(-J_a/kT)$; therefore, at too low temperatures, the time to reach thermodynamic equilibrium by the system may become too long in comparison with the characteristic time of the increase in the external field value from 0 to H_{c2} in the experiment [4]. On the contrary, at sufficiently high temperatures, a large number of thermally populated states effectively reduces the energy of the exchange interaction between chains, which is responsible for the formation of intermediate states. Switching between them occurs with a high frequency, which smooth the steps in the field dependence of magnetization. As a result, only two steps, H_{c1} and H_{c2}, remain observable, which correspond to structures with the largest energy difference [1]. The relaxation time of metastable states, as shown in [4], changes by 1000 times in the temperature range 2–3.5 K. Calculated activation energy $\Delta E/k = (33 \pm 5)$ K is close to the value of one "flipped" spin on the chain end, so the nucleation process occurs mainly on the sites of chain breaks.

The main feature of an electronic transition in Raman and IR absorption spectra is its response to an external magnetic field, in other words, the Zeeman effect. In our experiments, the CFC Raman spectra were studied in fields applied in the *a* and *c* directions in a magnetically ordered state. At this, various effects were observed: for one group of lines, this is the splitting in the field **H** ∥ *a* and the frequency shift in the field **H** ∥ *c*, in the rest it is a change in

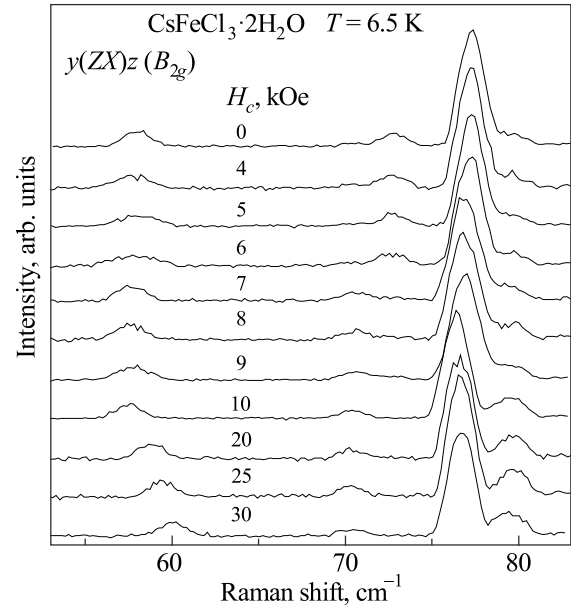*Fig. 3.* Evolution of a part of the CFC Raman spectrum in polarization *y*(*ZX*)*z* at a temperature 6.5 K in an external magnetic field **H** ∥ *c*. Spectral resolution 3 cm^{-1}.

the scattering intensity up to complete disappearance in the field **H** ∥ *c* and no response to the field **H** ∥ *a*. We assigned the first group to excitations of an electronic nature, and the further discussion is devoted to it.

4.2. Field dependence

Figure 3 shows the evolution of the low-frequency part of the CFC Raman spectrum, which in polarization corresponds to excitations with the B_{2g} symmetry within the crystal class *mmm*, at the temperature 6.5 K and the magnetic field direction **H** ∥ *c*. Also in the Fig. 4 the frequency dependence of the lines observed in this spectral region on the strength of the external field is presented. The characteristic features of individual lines behavior include:
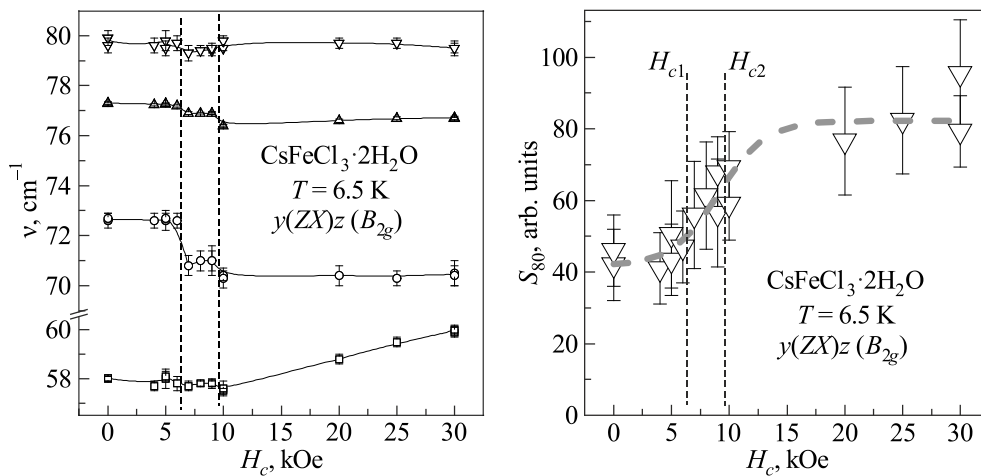

Fig. 4. The field dependence of the Raman lines frequencies, which are shown in Fig. 3, and the line 80 cm^{-1} area. The vertical dashed lines indicate the critical fields of metamagnetic transitions [1].

(1) The line with a frequency (frequencies are given for $H = 0$) 80 cm^{-1} does not suffer noticeable frequency changes, but shows a rise in its intensity, which nearly doubles in the field-induced F phase (right panel of Fig. 4). This line could be attributed to the missing phonon mode of B_{2g} symmetry, which is present in this frequency region of the spectrum in the isostructural CMC (see Table 3), but in the CFC its frequency exactly coincides with the frequency of the intense B_{3g} mode. The well-known effect of leakage of intense Raman lines into forbidden polarization, which has a geometric interpretation and is determined by the finiteness of the angular aperture of the receiving optics, sometimes causes difficulties in the identification of weak lines against their background. Such a scenario is implemented here.

The change in the intensity of the line at 80 cm^{-1} upon transition to the F phase can be an argument in favor of the fact that it is indeed a missing phonon mode with a vanishingly small Raman extinction at low temperatures. The transition to the F phase can lead, for example, to a change in the magnetic contribution to the scattering tensor. It was verified (not shown here) that the intensity of that supposedly leaking line of B_{3g} mode does not respond to the metamagnetic transition. Other optical phenomena that can change the leakage degree of the B_{3g} spectrum (for example, the Faraday rotation of the polarization of the exciting and scattered light in the Raman experiment) have not been detected. This fact is also confirmed by the invariability of the leakage degree of another intense B_{3g} 44.6 cm^{-1} line.

In addition to the dependence on the magnetic phase, the area of the discussed line B_{2g} 80 cm^{-1} exhibits an unusual temperature dependence [Fig. 5(b)]. Near T_N, the area of this line undergoes a sharp increase, similar to that observed during the transition to the F phase. Thus, it can be stated that the intensity of this supposedly phonon line is suppressed just in the AF phase, possibly due to the magnetic contribution to the Raman polarizability, which has the opposite sign with respect to the lattice polarizability [23]. By what manner this mechanism is realized for a given phonon remains an open question, since no visible interaction with the nearest in energy electronic transition was observed (see below).
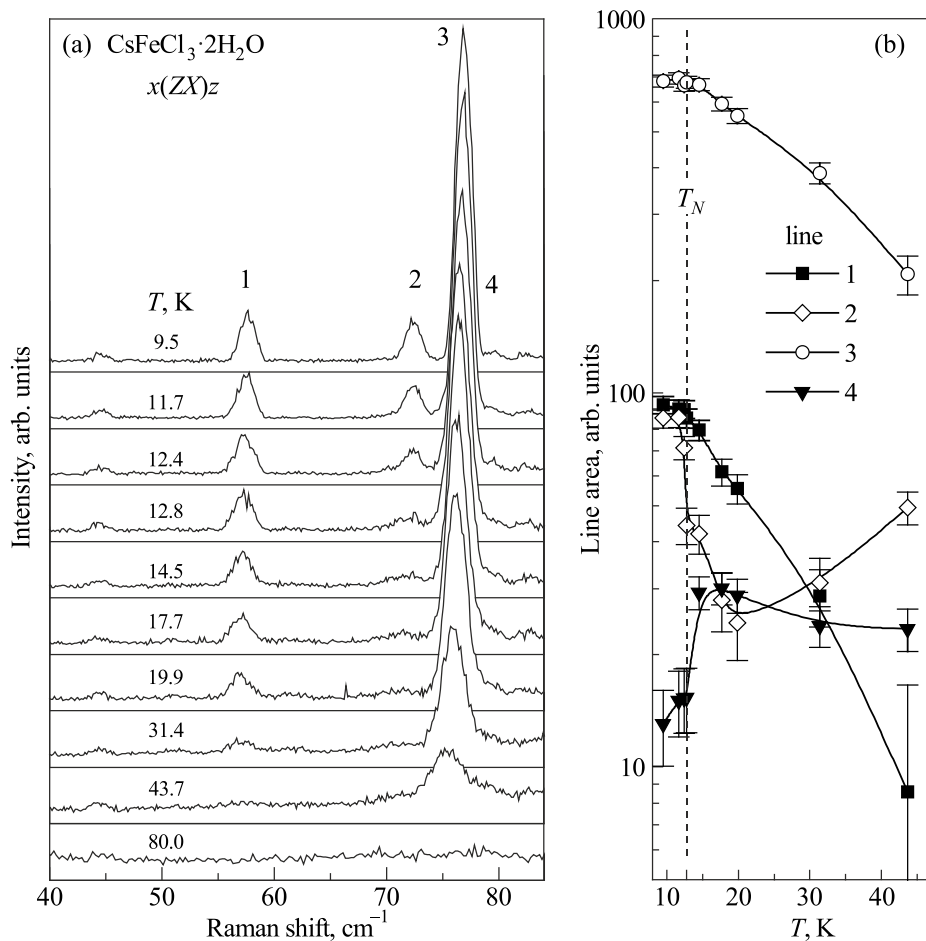

Fig. 5. (a) Temperature evolution of a part of the Raman spectrum of CFC with polarization $y(ZX)z$ in the energy range of the lowest electronic transitions. (b) Temperature dependence of the integral intensity of four lines of the spectrum. The dotted line marks T_N. Solid lines are eye guides. Spectral resolution 3 cm^{-1}.

(2) The 77 cm^{-1} line undergoes jumps in frequency in the fields H_{c1} and H_{c2}, which in our experiments are in good agreement with the literature data at 6.2 and 9.1 kOe [1, 4]. In a field $H_c > H_{c2}$, no noticeable change in frequency is observed. Only a very weak increase occurs with a rate of (0.016 ± 0.002) cm^{-1}/kOe. The temperature dependence of the area of this line is characteristic to electronic transitions. The integral intensity begins to decrease noticeably after T_N, but this decrease is exponential, which reflects a decrease in the magnetic correlations length in chains in the paramagnetic, from the point of view of the three-dimensional ordering, phase of CFC.

(3) The 73 cm^{-1} line, as well as the 77 cm^{-1} one, undergoes jumps in frequency in the H_{c1} and H_{c2} fields. However, these jumps are much larger; the overall decrease in the frequency of this line is more than 2.2 cm^{-1}. In the field $H_c > H_{c2}$, no more changes in frequency of the line are observed. An alternative description of the observed picture of the spectrum of the Raman spectrum modifications in the region of this weak line is also possible. A line with a frequency of 73 cm^{-1} disappears in the field H_{c2}, and another, with a frequency of 71 cm^{-1}, appears in a field of H_{c1}. The disappearance of the phonon line in the field H_{c2} is quite understandable from the point of view of restoring of the unit cell volume to the paramagnetic one as a result of the metamagnetic transition to the F phase. Such phonon lines are also observed in other parts of the spectrum [17].

The effect of "activation" of the second excitation in the phase F remains unclear in this interpretation. Also, the 73 cm^{-1} line differs from two neighboring ones in the behavior of the intensity with temperature (see Fig. 5). Its intensity rapidly decreases towards T_N (12.75 K) by about twice, while the lines at 77 and 58 cm^{-1} are observed up to temperatures of 40 K and higher. The reaction to T_N is similar to the 80 cm^{-1} line, but with the opposite sign.

(4) The most low-frequency line, 58 cm^{-1}, of the considering ones, undergoes a noticeable frequency shift in fields $H_c > H_{c2}$ with a rate of (0.128 ± 0.009) cm^{-1}/kOe. In low fields $H_c < H_{c2}$, according to IR studies [13], in the related RbFeCl$_3 \cdot$2H$_2$O, a splitting of a similar line is observed. At H_{c2}, it reaches no more than 2 cm^{-1}. Thus, this splitting is not detected in the Raman spectrum recorded with a resolution of 3 cm^{-1}. After the transition to the phase, when all sublattices have only a positive projection of the moments on the direction of the external magnetic field, the spectrum contains only one excited branch with increasing energy.

When an external field is applied along the crystallographic direction a, the picture changes; the so-called sublattice splitting is observed (Fig. 6). This behavior gives an unambiguous assignment of spectral lines 57 and 77 cm^{-1} to electronic transitions (lines 1 and 3 in Fig. 6). Transition 1 lowers its energy with increasing field H_a. Linear extrapolation leads to the value of the critical field $H_{a\,cr} = 157$ kOe, the field at which the transition energy reaches
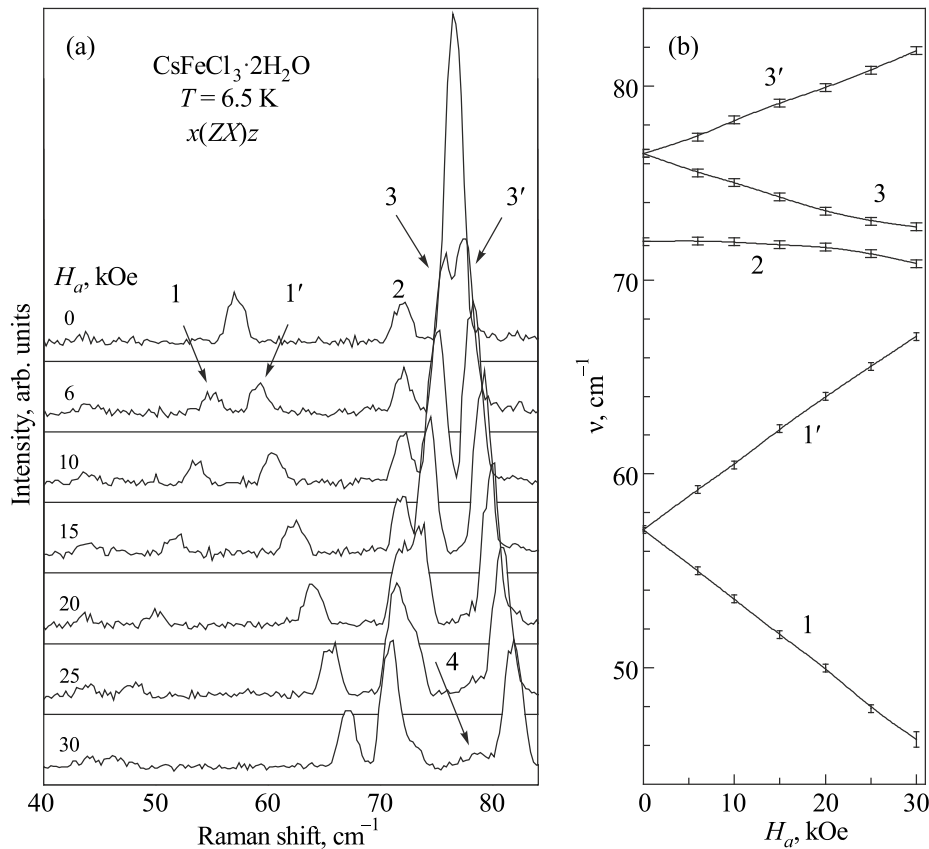

Fig. 6. (a) Evolution of a part of the CFC Raman spectrum in polarization $y(ZX)z$ at 6.5 K in an external magnetic field **H** $\parallel a$. (b) Field dependence of the frequencies of Raman lines. Spectral resolution 3 cm^{-1}.

zero. Taking into account the quadratic in the field correction, which leads to a decrease in the energy of the center of gravity of the 1 and 1′ transitions, gives the estimation of 134 kOe for this field. Experiments in strong stationary magnetic fields determined the metamagnetic transition at 140 kOe at 4.2 K [10], that is very close to the obtained estimates of the critical field, at which the ground state of magnetic ions changes in the sublattices with the opposite to the external magnetic field directions of the moments.

5. Discussion

To clarify the formation and further interpretation of the observed transformations of the electronic Raman spectra, in Fig. 7 a diagram of the energy levels of the discussed Ising antiferromagnetic system is presented. In this scheme, the lowest-energy line 57 cm^{-1} is associated with a transition between the components of the exchange-split quasi-doublet of the ground state — a spin-flip electronic transition, or a magnon in the Ising model. The next in energy transition refers to the excitation of the nearest singlet level from the ten lowest single-ion electronic states of Fe^{2+} in a tetragonally and rhombically distorted octahedral crystal field [21]. In the conventional terminology, such transitions are called excitonic, although their difference from magnons is conditional.

In the linear in field strength approximation, $\Delta E_{1',1}(H_a) = E_{1'}(H_a) - E_1(0) = \pm 2\mu_a H_a$. So, $E_{1'}(H_a) - E_1(H_a) = 4\mu_a H_a$ corresponds to the difference between energies of electronic transitions. The observed splitting of lines 1 and 1′, linear in the field, occurs at a rate of (0.7 ± 0.01) cm^{-1}/kOe, which corresponds to the modulus of the a-projections of the magnetic moments of the sublattices $\mu_a = (3.75 \pm 0.05)\,\mu_B$. It is interesting to note that under similar conditions in [13], the splitting of the IR spectral line in a frequency 50 cm^{-1} was observed. In the field $\mathbf{H} \parallel a$ with a strength 20 kOe, the splitting was $\Delta\nu = 14$ cm^{-1}, which exactly reproduces the scenario of the behavior of the 57 cm^{-1} Raman line in CFC. At that, the value of the magnetic moment in [13] was defined as $\mu = 4.2\,\mu_B$. Taking into account the canting of the magnetic moments relative to the direction a (see Table 1), and the behavior of the electron system is close to Ising-like, leads to the renormalization: $\mu_a = \mu \sin\theta$. For $\theta = 68°$, as it was given in [13], calculation results in $\mu_a = 3.89\,\mu_B$, that also does not correspond to the experiment.

The aforementioned shift of the 57 cm^{-1} line in the field $\mathbf{H} \parallel c$ in the F phase corresponds to the scheme for node i in Fig. 7. Here $\partial E/\partial H = 2\mu_c H_c$, whence $\mu_c = (1.37 \pm 0.1)\,\mu_B$. Basing on these values, the angle between the c axis and the directions of the magnetic moments of the sublattices can be calculated: it is $(70 \pm 2)°$. In Refs. 1, 4, the values $72-77°$ are occurred. The total magnetic moment obtained from our Raman data is $\mu = (4.0 \pm 0.1)\,\mu_B$.

It should be noted that different experimental methods lead to different estimates of the magnetic moment of the sublattices. For example, in $RbFeCl_3 \cdot 2H_2O$, this value varies
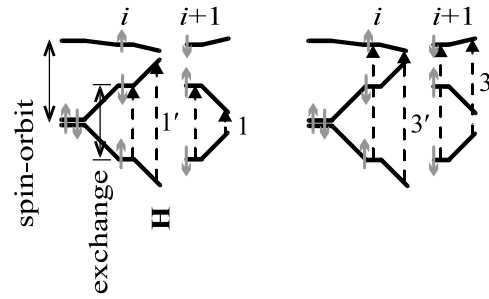

Fig. 7. Layout of the three lowest energy levels of two Fe^{2+} sublattices in a separate CFC chain. The indices i and $i + 1$ refer to neighboring sites with opposite projections of the magnetic moments onto the a axis in the ground state. The gray arrows conventionally denote the magnetic moments of these states. Dashed arrows show transitions between states without a field and in an external field $\mathbf{H} \parallel a$. The numbers indicate the transitions corresponding to the lines of the spectra in Fig. 6.

from 3.9 to 4.5 μ_B (see [13] and the references therein). In the CFC, the estimate of the saturation magnetic moment upon the transition to the spin-flip phase according to the data of [10, 22] is $\mu_a = 4.1\,\mu_B$. The authors of [22] believe that complete saturation is achieved in a field of 200 kOe. If the canting angle of the moments with respect to the a axis (Ising anisotropy) for $\theta = 70°$ is preserved, the total moment of the sublattice is $\mu = 4.36\,\mu_B$ at 4.2 K.

The splitting of the 77 cm^{-1} line in CFC in the H_a field occurs at a much slower rate. The range of field strengths from 0 to 15 kOe is selected for the assessment. At high strengths, as can be seen in Fig. 6, the softening branch 3 interacts with the 73 cm^{-1} phonon mode. The increasing branch 3′ demonstrates a linear increase in frequency up to 35 kOe, crossing the supposedly phonon line 80 cm^{-1} without noticeable interaction [line 4 in Fig. 6(a)]. In accordance with the diagram in Fig. 7, the field dependence of the 3 and 3′ transitions is described by the expression $E_{3,3'}(H_a) = E_3(0) \mp (\mu_a - \mu'_a)H_a$, where μ'_a is the projection of the moment of the singlet level onto the a axis. Accordingly, $\mu'_a = \mu_a - [E_{3'}(H_a) - E_3(H_a)]/2H_a = (0.34 \pm 0.14)\mu_B$. The magnetic moment of this level, as expected [12], is about one order of magnitude less than the moment in the ground state, but its calculated value exceeds the confidence interval of the determination error. The almost complete absence of the frequency dependence of this transition if the field is applied in the direction of the c axis indicates the proximity of the projections $\mu'_c = (1.0 \pm 0.3)\mu_B \approx \mu_c$. This means that in an excited state the moment is oriented differently than in the ground one, or the g-factor of this state has no longer the Ising character.

The studies in magnetic field were carried out in the *ZX* polarization, where the lines of the Raman spectrum corresponding to electronic transitions have the maximum intensity. An analysis of the polarization selection rules for magnons, i.e., excitations within the exchange-split Ising

quasi-doublet, showed that acoustic magnons should be observed in the *XZ* (or *ZX*) and *XY* (or *YX*) components of the scattering tensor. Exchange magnons associated with the 8-sublattice antiferromagnetic structure of the CFC are allowed in the off-diagonal *YZ* or *ZY* and diagonal *XX*, *YY*, *ZZ* components of the scattering tensor. In reality, weak Raman lines of electronic origin in the low-frequency (magnon) region of the spectrum are observed only in the off-diagonal components. The 57 cm^{-1} magnon band discussed above is presented in the *XZ* (or *ZX*) and *XY* (or *YX*) polarizations. The 77 cm^{-1} exciton transition line obeys the same observation rules, which is consistent with the theoretically predicted values.

6. Conclusions

The frequencies of the lowest electronic excitations of 57 and 77 cm^{-1} have been determined, the first of which refers to the magnon in the Ising model of the ground state of paramagnetic Fe^{2+} ions in CFC. The second, most likely, refers to an exciton excitation associated with the transition to the lowest excited level of the spin multiplet of the orbital quasi-doublet d_{zx}, d_{zy} split by the spin-orbit interaction. From the frequency shifts and line splitting in external fields applied along the crystallographic directions *a* and *c*, the magnetic moment of the sublattices is estimated as (4.0 ± 0.1) μ_B; and the angle between the direction of *c* axis and the magnetic moments in the ground state is $(70 \pm 2)°$.

———

1. J. A. J. Basten, Q. A. G. van Vlimmeren, and W. J. M. de Jonge, *Phys. Rev. B* **18**, 2179 (1978).
2. S. J. Jensen, P. Andersen, and S. R. Rasmussen, *Acta Chem. Scand.* **16**, 1890 (1962).
3. N. Thorup and H. Soling, *Acta Chem. Scand.* **23**, 2933 (1969).
4. J. P. M. Smeets, E. Frikkee, W. J. M. de Jonge, and K. Kopinga, *Phys. Rev. B* **31**, 7323 (1985).
5. C. H. W. Swüste, W. J. M. de Jonge, and J. A. G. W. van Meijel, *Physica* **76**, 21 (1974).
6. R. D. Spence, W. J. M. de Jonge, and K. W. S. Rama Rao, *J. Chem. Phys.* **51**, 4694 (1969).
7. W. J. M. de Jonge and C. H. W. Swüste, *J. Chem. Phys.* **61**, 4981 (1974).
8. A. Herweijer, W. J. M. de Jonge, A. C. Botterman, A. L. M. Bongaarts, and J. A. Cowen, *Phys. Rev. B* **5**, 4618 (1972).
9. K. Kopinga, M. Steiner, and W. J. M. de Jonge, *J. Phys. C* **18**, 3511 (1985).
10. M. Takeda, G. Kido, I. Mogi, Y. Nakawaga, H. Okada, and N. Kojima, *J. Phys. Soc. Jpn.* **58**, 3418 (1989).
11. I. Mogi, M. Takeda, G. Kido, Y. Nakawaga, H. Okada, and N. Kojima, *J. Magn. Magn. Mater.* **104–107**, 1061 (1992).
12. H. Okada, N. Kojima, T. Ban, and I. Tsujikawa, *Phys. Rev. B* **42**, 11610 (1990); H. Okada, N. Kojima, T. Ban, I. Tsujikawa, *Phys. Rev. B* **42**, 11619 (1990).
13. Q. A. G. van Vlimmeren, C. H. W. Swüste, W. J. M. de Jonge, M. J. H. van der Steeg, J. H. M. Stoelinga, and P. Vyder, *Phys. Rev. B* **21**, 3005 (1980).
14. D. M. Adams and D. Newton, *J. Chem. Soc. A* **22**, 3499 (1971).
15. V. P. Gnezdilov, V. V. Eremenko, V. S. Kurnosov, and V. I. Fomin, *Fiz. Nizk. Temp.* **17**, 630 (1991) [*Sov. J. Low Temp. Phys.* **17**, 331 (1991)].
16. W. Jia, E. Strauss, W. M. Yen, K. Xia, and M. Zhao, *Phys. Rev. B* **39**, 12853 (1989).
17. V. S. Kurnosov, A. V. Peschanskii, V. I. Fomin, A. V. Yeremenko, and Yu. G. Pashkevich, *Fiz. Nizk. Temp.* **28**, 724 (2002) [*Low Temp. Phys.* **28**, 516 (2002)].
18. V. Tkáč, K. Tibenska, A. Orendáčova, M. Orendáč, J. Šebek, V. Sechovský, A. G. Anders, V. Pavlík, and A. Feher, *Phys. Status Solidi B* **248**, 2834 (2011).
19. T. C. Damen, S. P. S. Porto, and B. Tell, *Phys. Rev.* **142**, 570 (1966).
20. V. Eremenko, V. Fomin, and V. Kurnosov, *J. Magn. Magn. Mater.* **157–158**, 484 (1996).
21. H. Th. Le Fever, R. C. Thiel, W. J. Huiskamp, and W. J. M. de Jonge, *Physica B* **111**, 190 (1981).
22. M. Takeda, G. Kido, Y. Nakagawa, H. Okada, N. Kojima, and I. Tsujikawa, *J. de Phys. (Paris)* **49**, C8-1461 (1988).
23. N. Suzuki and H. Kamimura, *J. Phys. Soc. Jpn.* **35**, 985 (1973).

———

Дослідження низькоенергетичних електронних збуджень в квазіодновимірному ізінгівському антиферомагнетику CsFeCl$_3$·2H$_2$O методом раманівської спектроскопії

V. S. Kurnosov

Частоти низьколежачих електронних збуджень у квазіодновимірному антиферомагнетику CsFeCl$_3$·2H$_2$O визначено методом раманівської спектроскопії. Найнижче з них (57 см$^{-1}$) асоційовано із магноноподібним збудженням у ланцюжку ізінгівських спінів парамагнітних іонів Fe^{2+}. А наступне (77 см$^{-1}$), найбільш вірогідно, може бути віднесеним до ексітоноподібного збудження, яке пов'язано з електронним переходом на нижній рівень збудженого орбітального квазідублету d_{zx}, d_{zy}, що є розщепленим спін-орбітальною взаємодією. Дослідження розщеплень та частотних зсувів раманівських ліній у зовнішньому магнітному полі дозволили оцінити величини магнітних моментів підграток в основному стані та визначити їх просторову орієнтацію відносно кристалографічних напрямків.

Ключові слова: магнон, ексітон, ізінгівський спіновий ланцюжок, квазіодновимірний антиферомагнетик.